

Quasifree eta photoproduction from nuclei and medium modifications of resonances

B.I.S. van der Ventel,^{1,*} L. J. Abu-Raddad,^{2,3} and G.C. Hillhouse^{1,2}

¹*Department of Physics, University of Stellenbosch, Stellenbosch 7600, South Africa*

²*Research Center for Nuclear Physics, Osaka University,*

10-1 Mihogaoka, Ibaraki, Osaka 567-0047, Japan

³*Department of Infectious Disease Epidemiology,*

Imperial College Faculty of Medicine, St Mary's Campus,

Norfolk Place, London W2 1PG, United Kingdom

(Dated: October 25, 2018)

Abstract

This article establishes the case that the process of quasifree η photoproduction from nuclei is a prized tool to study medium modifications and changes to the elementary process $\gamma N \rightarrow \eta N$ in the nuclear medium. We investigate the sensitivity of the differential cross section, recoil nucleon polarization and the photon asymmetry to changes in the elementary amplitude, medium modifications of the resonance (S_{11}, D_{13}) masses, as well as nuclear target effects. All calculations are performed within a relativistic plane wave impulse approximation formalism resulting in analytical expressions for all observables. Our results indicate that polarization observables are largely insensitive to nuclear target effects. Depending on the type of coupling, the spin observables do display a sensitivity to the magnitude of the ηNN coupling constant. The polarization observables are identified to be the prime candidates to investigate the background processes and their medium modifications in the elementary process such as the D_{13} resonance. Moreover, as a consequence of the large dominance in the differential cross section of the S_{11} resonance, the quasifree differential cross section provides an exceptional instrument to study medium modifications to the S_{11} resonance in such a manner that helps to distinguish between various models that attempt to understand the S_{11} resonance and its distinctive position as the lowest lying negative parity state in the baryon spectrum.

PACS numbers: 25.20.-x, 25.20.Lj, 13.60.Le, 14.40.Aq, 24.10.Jv

*Electronic address: bventel@sun.ac.za

I. INTRODUCTION

The η electro- and photoproduction processes continue to enjoy significant investigations from a variety of approaches. This interest stems from the fact that η processes form a gate to understand several fundamental puzzling issues in nuclear and particle physics today such as measuring the $\bar{s}s$ quark content in the nucleon [1]. While the η photoproduction process is only one of many meson photoproduction processes from nuclei, the characteristic reactive content of this process near threshold provides it with a distinguished role among other meson photoproduction processes. Part of the reason is that the interaction is dominated cleanly by only one resonance near threshold. This is the $S_{11}(1535)$ resonance with its peculiar status as the lowest lying negative parity resonance in the baryon spectrum. Favorably, the theoretical interest has been correlated with experimental advances, particularly with the construction and running of modern electron-scattering facilities, such as the Thomas Jefferson National Accelerator Facility (JLab) and Mainz [2, 3].

Understanding the structure of the S_{11} resonance is of prime interest in baryon physics as it is believed that this resonance plays a crucial role in the dynamics of chiral symmetry and its spontaneous breaking in the baryon spectrum. The S_{11} resonance has been studied using various approaches including effective Lagrangian theory [4, 5, 6, 7, 8] and QCD sum rules [9, 10, 11, 12]. Yet, a more unifying approach is to study this resonance using chiral symmetry and its spontaneous breaking and restoration. Indeed, DeTar and Kunihiro have suggested the “mirror assignment” of chiral symmetry where the S_{11} resonance, as the lowest lying negative parity resonance, is the chiral partner of the nucleon and transforms in an opposite direction compared to the nucleon [13]. However, Jido, Nemoto, Oka, and Hosaka have suggested a different realization of chiral symmetry through what they label as the “naïve assignment” [14, 15]. Improvements to these models have been suggested through the inclusion of nonlinear terms that preserve chiral symmetry [16]. Understanding the medium modifications of the S_{11} resonance will help us discriminate between the different models of chiral symmetry assignment, and in turn, this leads us to understanding the structure of this resonance and the prediction of its properties under chiral symmetry restoration.

It had been thought earlier that the coherent η photoproduction process from nuclei may in fact help us to study the medium modifications of the S_{11} resonance [17]. Nonetheless, it has been shown that the S_{11} contribution, although dominant for the elementary process

$\gamma N \rightarrow \eta N$, is strongly suppressed in the coherent process due to the filtering of only the isoscalar contribution and due to the spin-flip nature of the S_{11} exchange diagram [18, 19, 20]. Hence, the η process $A(\gamma, \eta N)B$ in the quasifree regime, with its strong dependence on the resonance contribution, provides an opportunity to understand the medium modifications of the S_{11} resonance.

Building on a series of η photoproduction studies [21, 22, 23, 24, 25, 26, 27], Lee, Wright, Bennhold, and Tiator studied the η quasifree process using the nonrelativistic distorted wave impulse approximation (DWIA) formalism [28]. In this work, we also assume the impulse approximation but provide a fully relativistic study in both the reactive content and the nuclear structure. Furthermore, we use a different and robust dynamical content for the elementary process [6, 29, 30] and study this process in a different kinematic setting compared to the one used by Lee *et al.* Our article constitutes the third application of our established quasifree formalism [31] after studying the kaon [32] and the electron [33] quasifree reactions. The goal here is to shed light on the elementary process $\gamma N \rightarrow \eta N$ by furnishing a different physical setting from the on-shell point for studying the elementary amplitude. We also examine the possibility of using this process to extract medium modification effects to the propagation of the S_{11} and D_{13} resonances. We provide special attention in our work to the polarization observables, the recoil polarization of the ejected nucleon and the photon asymmetry, as they are very sensitive to the fine details in the reactive content and are effective discriminators of subtle physical effects compared to the unpolarized differential cross section. Moreover, the quasifree polarization observables, while very sensitive to the fundamental processes, are insensitive to distortion effects [28, 34, 35]. Finally, by comparing against the polarization observables of the free process, medium effects can be discerned.

The effects of relativity in meson quasifree processes are still not well understood. While it appears that the polarization observables are not sensitive to the enhanced lower component of the Dirac spinors in the relativistic nuclear structure models [32], other results indicate important differences compared to nonrelativistic Schrödinger-based formalisms. Relativistic plane-wave impulse approximation (RPWIA) calculations, such as the one we present in this study, have identified subtle dynamics not present at the nonrelativistic level. Two notable examples to quote here are that relativistic effects contaminate any attempt to infer color transparency from a measurement of the asymmetry in the $(e, e'p)$ reaction [36] and the breakdown of the nonrelativistic factorization picture in the $(e, e'p)$ process as a consequence

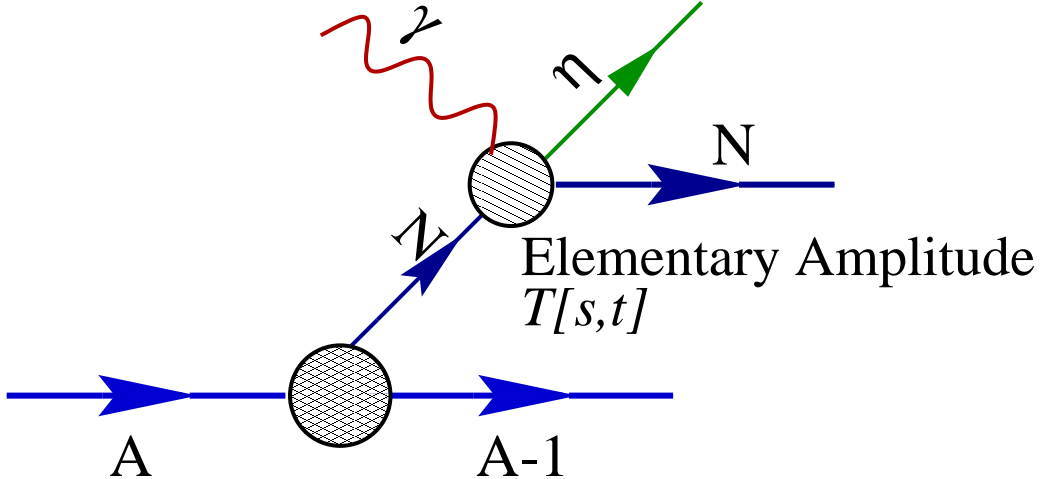


FIG. 1: A schematic diagram of the η meson quasifree photoproduction within the framework of a plane-wave impulse-approximation approach.

of the presence of negative-energy components in the bound-nucleon wave function [37].

Although processes of η photoproduction from nucleons and nuclei have recently enjoyed significant experimental attention, the current experimental work for quasifree scattering has thus far been limited to the measurement of the total and differential cross sections. This includes scattering off the deuteron [3] and ${}^4\text{He}$ [38, 39] as well as heavier nuclei [40]. Nonetheless what is theoretically desired are measurements of the polarization observables as these observables continue to show the promise of discerning the subtle dynamics in meson photoproduction processes. With the advent of JLab and Mainz such measurements are finally realizable.

We have organized our paper as follows. In Sec. II we discuss our relativistic plane-wave formalism, placing special emphasis on the use of the “bound-nucleon propagator” to enormously simplify the formalism. In Sec. III, this formalism is applied to calculate the unpolarized differential cross section, the recoil nucleon polarization and the photon asymmetry. Finally, conclusions are drawn in Sec. IV.

II. FORMALISM

A. Kinematic constraints

In the meson quasifree photoproduction $A(\gamma, \eta N)B$, the kinematics are constrained by two conditions. The first is an overall energy-momentum conservation:

$$k + p_A = k' + p' + p_B . \quad (1)$$

Here k is the four-momentum of the incident photon, while k' and p' are the momenta of the produced η and nucleon, respectively. $p_A(p_B)$ represents the momentum of the target (recoil) nucleus. Since we assume the impulse approximation, as shown in Fig. 1, another kinematical constraint emerges from the energy-momentum conservation at the $\gamma N \rightarrow \eta N$ vertex:

$$k + p = k' + p' , \quad (2)$$

where p is the four-momentum of the bound nucleon, whose spatial part is known in the literature as the missing momentum

$$\mathbf{p}_m \equiv \mathbf{p}' - \mathbf{q} ; \quad (\mathbf{q} \equiv \mathbf{k} - \mathbf{k}') . \quad (3)$$

The dependence of the cross section on the missing momentum (See Section III) results in the interaction becoming a probe of the nucleon momentum distribution, just as in most semi-inclusive processes, one of which is the $(e, e' p)$ reaction [33].

B. Cross section and polarization observables

Using the conventions of Bjorken and Drell [41], the differential cross section for the scattering process depicted in Fig. 1 is given by

$$\left(\frac{d^5\sigma(s', \varepsilon)}{d\mathbf{k}' d\Omega_{\mathbf{k}'} d\Omega_{\mathbf{p}'} } \right)_{\text{lab}} = \frac{2\pi}{2E_\gamma} \frac{|\mathbf{k}'|^2}{(2\pi)^3 2E_{\mathbf{k}'}} \frac{M_N |\mathbf{p}'|}{(2\pi)^3} |\mathcal{M}|^2 , \quad (4)$$

where s' is the spin of the emitted nucleon, ε is the polarization of the incident photon, M_N is the nucleon mass, and \mathcal{M} is the scattering matrix element defined as

$$|\mathcal{M}|^2 = \sum_m \left| \bar{\mathcal{U}}(\mathbf{p}', s') T(s, t) \mathcal{U}_{\alpha, m}(\mathbf{p}) \right|^2 . \quad (5)$$

Note that $\mathcal{U}(\mathbf{p}', s')$ is the free Dirac spinor for the knocked-out nucleon while $\mathcal{U}_{\alpha,m}(\mathbf{p})$ is the Fourier transform of the relativistic spinor for the bound nucleon (α stands for the collection of all quantum numbers of the single-particle orbital). The use of the impulse approximation is evident in this expression where we invoke the on-shell photoproduction operator $T(s, t)$.

By summing over the two spin components of the emitted nucleon and averaging over the transverse photon polarization in Eq. (4), we obtain an expression for the unpolarized differential cross section

$$\left(\frac{d^5\sigma}{d\mathbf{k}'d\Omega_{\mathbf{k}'}d\Omega_{\mathbf{p}'}} \right)_{\text{lab}} = \frac{1}{2} \sum_{s', \varepsilon} \left(\frac{d^5\sigma(s', \varepsilon)}{d\mathbf{k}'d\Omega_{\mathbf{k}'}d\Omega_{\mathbf{p}'}} \right)_{\text{lab}} . \quad (6)$$

Nonetheless, our main interest is in the polarization observables as they are the true discriminators of subtle dynamics. Hence, the recoil nucleon polarization (\mathcal{P}) is given by [42, 43]

$$\mathcal{P} = \sum_{\varepsilon} \left(\frac{d^5\sigma(\uparrow) - d^5\sigma(\downarrow)}{d^5\sigma(\uparrow) + d^5\sigma(\downarrow)} \right)_{\text{lab}} , \quad (7)$$

while the photon asymmetry (Σ) is provided through the expression [28, 35]

$$\Sigma = \sum_{s'} \left(\frac{d^5\sigma(\perp) - d^5\sigma(\parallel)}{d^5\sigma(\perp) + d^5\sigma(\parallel)} \right)_{\text{lab}} . \quad (8)$$

Here the \uparrow and \downarrow represent the projection of the spin of the nucleon with respect to the normal to the scattering plane ($\mathbf{k} \times \mathbf{k}'$), while \perp (\parallel) represents the out-of-plane (in-plane) polarization of the photon.

C. Elementary ($\gamma p \rightarrow \eta N$) Amplitude

We use the canonical model-independent parameterization for the elementary process $\gamma p \rightarrow \eta N$. This parameterization is constructed in terms of four Lorentz- and gauge-invariant amplitudes [21, 44, 45]

$$T(\gamma p \rightarrow \eta N) = T(s, t) = \sum_{i=1}^4 A_i(s, t) M_i , \quad (9)$$

where the invariant matrices have been defined as:

$$M_1 = -\gamma^5 \not{k} , \quad (10a)$$

$$M_2 = 2\gamma^5 [(\varepsilon \cdot p)(k \cdot p') - (\varepsilon \cdot p')(k \cdot p)] , \quad (10b)$$

$$M_3 = \gamma^5 [\not{\varepsilon}((k \cdot p) - \not{k}(\varepsilon \cdot p))] , \quad (10c)$$

$$M_4 = \gamma^5 [\not{\varepsilon}((k \cdot p') - \not{k}(\varepsilon \cdot p'))] . \quad (10d)$$

One must stress here that although this parameterization is conventional, it is certainly not unique. Many other parameterizations, which are all equivalent for on-shell spinors, are possible [20]. The problem is that in the quasifree process the bound nucleon is off its mass shell and these various parameterizations may no longer be equivalent off-shell. While one can use a specific model for the η photoproduction process which fixes the off-shell behavior of these amplitudes, this still does not solve the problem of medium modifications as the driving dynamics, such as the S_{11} resonance, may change its properties in the nuclear medium. The problem can be addressed by modeling how the propagation in the nuclear medium affects the inherent dynamics. Such models, however, can be very different in their predictions (See Section I) which makes the quasifree process an ideal candidate to distinguish between them.

It is more convenient at this stage to transform the above parameterizations to a form that shows explicitly the Lorentz and parity structure of the amplitude as given by [18, 20]

$$T(\gamma p \rightarrow \eta N) = F_T^{\alpha\beta} \sigma_{\alpha\beta} + iF_P \gamma_5 + F_A^\alpha \gamma_\alpha \gamma_5 , \quad (11)$$

where the tensor, pseudoscalar, and axial-vector amplitudes are defined through

$$F_T^{\alpha\beta} = \frac{1}{2} \varepsilon^{\mu\nu\alpha\beta} \varepsilon_\mu k_\nu A_1(s, t) , \quad (12a)$$

$$F_P = -2i \left[(\varepsilon \cdot p)(k \cdot p') - (\varepsilon \cdot p')(k \cdot p) \right] A_2(s, t) , \quad (12b)$$

$$F_A^\alpha = \left[(\varepsilon \cdot p)k^\alpha - (k \cdot p)\varepsilon^\alpha \right] A_3(s, t) + \left[(\varepsilon \cdot p')k^\alpha - (k \cdot p')\varepsilon^\alpha \right] A_4(s, t) . \quad (12c)$$

While this parameterization is model independent, one still needs to determine the four Lorentz and gauge invariant amplitudes $A_i(s, t)$. In principle one can just extract them experimentally or use some other formalism that calculates these amplitudes based on effective Lagrangian theory or other approaches. Here we use the effective Lagrangian approach of Benmerrouche, Zhang, and Mukhopadhyay (BZM) [6, 29, 30]. Such an approach is more fundamental and satisfies stringent theoretical constraints compared to other treatments such as Breit-Wigner-type parameterizations [46, 47] or coupled channel isobar models [21, 25, 28]. The BZM treatment is specially distinguished by the limited number of free parameters (a maximum of eight) compared to other models.

The BZM approach we adopt here, includes spin-1/2 [$S_{11}(1535)$] and spin-3/2 [$D_{13}(1520)$] resonances as well as nucleon Born terms and vector meson exchanges (ω and ρ). All free parameters in the model were determined by fitting the experimental data for $p(\gamma, \eta)p$ [2]

and $d(\gamma, \eta)pn$ [3]. The cross section is clearly dominated by the S_{11} resonance in this model. However, there are still important and necessary contributions, particularly in the angular distributions, from the D_{13} resonance, nucleon born terms, and vector meson exchanges.

D. Nuclear-Structure Model

We use in this work a relativistic mean-field approximation to the Walecka model [48] for all calculations of nuclear structure. In the case of nuclei with spherically symmetric potentials such as those studied here, the Dirac bound-state spinors can be classified with respect to a generalized angular momentum κ [49]. These states can be expressed in a two-component representation according to

$$\mathcal{U}_{E\kappa m}(\mathbf{x}) = \frac{1}{x} \begin{bmatrix} g_{E\kappa}(x) \mathcal{Y}_{+\kappa m}(\hat{\mathbf{x}}) \\ i f_{E\kappa}(x) \mathcal{Y}_{-\kappa m}(\hat{\mathbf{x}}) \end{bmatrix}, \quad (13)$$

where the spin-angular functions are defined as:

$$\mathcal{Y}_{\kappa m}(\hat{\mathbf{x}}) \equiv \langle \hat{\mathbf{x}} | l_{\frac{1}{2}} j m \rangle; \quad j = |\kappa| - \frac{1}{2}; \quad l = \begin{cases} \kappa, & \text{if } \kappa > 0; \\ -1 - \kappa, & \text{if } \kappa < 0. \end{cases} \quad (14)$$

The Fourier transform of the relativistic bound-state spinor is given by

$$\mathcal{U}_{E\kappa m}(\mathbf{p}) \equiv \int d\mathbf{x} e^{-i\mathbf{p}\cdot\mathbf{x}} \mathcal{U}_{E\kappa m}(\mathbf{x}) = \frac{4\pi}{p} (-i)^l \begin{bmatrix} g_{E\kappa}(p) \\ f_{E\kappa}(p)(\sigma \cdot \hat{\mathbf{p}}) \end{bmatrix} \mathcal{Y}_{+\kappa m}(\hat{\mathbf{p}}), \quad (15)$$

where we have written the Fourier transforms of the radial wave functions as

$$g_{E\kappa}(p) = \int_0^\infty dx g_{E\kappa}(x) \hat{j}_l(px), \quad (16a)$$

$$f_{E\kappa}(p) = (\text{sgn}\kappa) \int_0^\infty dx f_{E\kappa}(x) \hat{j}_{l'}(px). \quad (16b)$$

The Riccati-Bessel function is incorporated here in terms of the spherical Bessel function $\hat{j}_l(z) = z j_l(z)$ [50]. The l' is the orbital angular momentum corresponding to $-\kappa$ as given in Eq. (14).

E. Closed-form Expression for the Photoproduction Amplitude

Having discussed some of the basic elements of our formalism, the next step is to calculate the square of the photoproduction amplitude [Eq. (5)]. In doing so we use the relativistic

plane wave impulse approximation and incorporate no distortions for the emitted nucleon or η . Our rationale is that we concentrate on the polarization observables as they are true discriminators of the subtle dynamics. Fortunately, these observables, although very sensitive to the elementary amplitude dynamics, are strikingly insensitive to distortions as has been suggested by several nonrelativistic studies [28, 34, 35]. Consequently, it is straightforward to evaluate the knocked-out nucleon propagator using the Casimir “trick”:

$$S(p') \equiv \sum_{s'} \mathcal{U}(\mathbf{p}', s') \overline{\mathcal{U}}(\mathbf{p}', s') = \frac{\not{p}' + M_N}{2M_N} ; \quad \left(p'^0 \equiv E_N(\mathbf{p}') = \sqrt{\mathbf{p}'^2 + M_N^2} \right) . \quad (17)$$

Gardner and Piekarewicz [31, 32, 36] have shown that a similar procedure holds even for bound-state spinors where the “bound-state propagator” can be cast in the form

$$\begin{aligned} S_\alpha(\mathbf{p}) &\equiv \frac{1}{2j+1} \sum_m \mathcal{U}_{\alpha,m}(\mathbf{p}) \overline{\mathcal{U}}_{\alpha,m}(\mathbf{p}) \\ &= \left(\frac{2\pi}{p^2} \right) \begin{pmatrix} g_\alpha^2(p) & -g_\alpha(p)f_\alpha(p)\sigma \cdot \hat{\mathbf{p}} \\ +g_\alpha(p)f_\alpha(p)\sigma \cdot \hat{\mathbf{p}} & -f_\alpha^2(p) \end{pmatrix} \\ &= (\not{p}_\alpha + M_\alpha) , \quad \left(\alpha = \{E, \kappa\} \right) . \end{aligned} \quad (18)$$

Note that we have defined the above mass-, energy-, and momentum-like quantities as

$$M_\alpha = \left(\frac{\pi}{p^2} \right) [g_\alpha^2(p) - f_\alpha^2(p)] , \quad (19a)$$

$$E_\alpha = \left(\frac{\pi}{p^2} \right) [g_\alpha^2(p) + f_\alpha^2(p)] , \quad (19b)$$

$$\mathbf{p}_\alpha = \left(\frac{\pi}{p^2} \right) [2g_\alpha(p)f_\alpha(p)\hat{\mathbf{p}}] , \quad (19c)$$

which satisfy the “on-shell relation”

$$p_\alpha^2 = E_\alpha^2 - \mathbf{p}_\alpha^2 = M_\alpha^2 . \quad (20)$$

This algebraic trick results in an enormous simplification in the formalism due to the similarity in structure between the free and bound propagators [Eqs. (17) and (18)]. The calculation of the square of the photoproduction amplitude boils down to an evaluation of traces of γ -matrices. This simplification would have not been possible had we incorporated distortion effects for the emitted nucleon.

In evaluating the ensuing traces of γ matrices, we are greatly aided by the use of *FeynCalc* package [51] with *Mathematica*. The tedious work of calculating, analytically, the tens

of traces of γ matrices can be borne by the computer and eventually we arrive elegantly at transparent analytical results for all observables. The results can then be fed into a FORTRAN code to obtain the final numerical values for all observables in the problem.

III. RESULTS AND DISCUSSION

There are many ingredients, mostly related to the nature of the model used for the elementary process, that go into the calculation of the observables for quasifree η photoproduction.

In our treatment, the basic ingredients are the Born and vector meson terms, the S_{11} and D_{13} resonances, as well as the coupling constants and the choice of pseudoscalar or pseudovector coupling at the meson-nucleon vertex. In the subsequent sections we investigate the sensitivity of the observables to variations in the elementary amplitude, medium modifications to the masses of the S_{11} and D_{13} resonances as well as to different nuclear targets. All calculations are done not far from threshold at an incident photon laboratory kinetic energy of 750 MeV.

In Ref. [28] a nonrelativistic distorted wave model of quasifree η photoproduction was given. In the previous section we presented a fully relativistic formalism, but using the plane wave approximation for the nucleon and η . While distortions are very difficult to incorporate in an analytical relativistic treatment such as ours, they do not appear to have any significance apart from quenching the cross section in such a manner that does not affect polarization observables. Indeed, the spin observables although very sensitive to the elementary amplitude dynamics, are insensitive to distortions at least as far as the η photoproduction process is concerned [28, 34, 35]. We will therefore pay special attention to these observables in all subsequent sections.

A. Sensitivity to variations in the elementary amplitude

It is clear from Eqs. (4) and (6)-(8) that the unpolarized differential cross section, the recoil nucleon polarization and the photon asymmetry are determined by the scattering matrix element \mathcal{M} . Eq. (5) in turn shows that one of the primary ingredients in the calculation of \mathcal{M} is the interaction matrix $T(s, t)$. From Eq. (9) we see that it is determined by the four invariant amplitudes $A_i(s, t)$. These amplitudes contain the dynamics of the reaction.

In this work the effective Lagrangian model of Benmerrouche, Zhang and Mukhopadyay [6, 29, 30] is used to determine the dynamics where the elementary process depends on four key components: (i) the nucleon Born terms, (ii) the vector mesons (ω and ρ) exchange, (iii) the S_{11} resonance and (iv) the D_{13} resonance. The contributions from other vector mesons such as the ϕ or other heavier mesons are shown to be negligible as a consequence of several reasons including the Okubo-Zweig-Iizuka suppression, the largeness of masses, and the meager coupling to the photoproduction channel [6]. Furthermore, the contributions from other resonances are insignificant primarily due to their larger masses or small coupling to the ηN channel in the energy regime of interest (near threshold) [6]. In this section we investigate how each of these four components influence the measured observables. All results in this section were obtained for proton knockout from the $1p^{3/2}$ orbital of ^{12}C , apart from the results in Fig. 4 which refer to neutron knockout from the same orbital. All calculations were done for an incident photon laboratory kinetic energy, $E_\gamma = 750$ MeV, while the missing momentum was fixed at $|\vec{p}_m| = 100$ MeV. This value of $|\vec{p}_m|$ is near the peak of the momentum distribution of the bound nucleon, i.e., where the cross section is maximized. Except for Fig. 5, all calculations employed pseudoscalar coupling at the ηNN vertex.

In Fig. 2 we show calculations of the unpolarized differential cross section ($d^5\sigma/dk'd\Omega_{k'}d\Omega_{p'}$), the recoil nucleon polarization (\mathcal{P}) and the photon asymmetry (Σ) for proton knockout from the $1p^{3/2}$ orbital of ^{12}C as a function of the η meson scattering angle, θ_η . In this figure the solid line represents the full calculation where all four components of the effective Lagrangian model are used in the evaluation of the invariant amplitudes $A_i(s, t)$. The dashed line represents the calculation using only the S_{11} resonance. Fig. 2 clearly displays that the S_{11} resonance gives the dominant contribution to the unpolarized quasifree differential cross section just as in the elementary reaction. This is in contrast to coherent η photoproduction where the contribution of this resonance is strongly suppressed due to the filtering of the isoscalar component and the spin-flip nature of the S_{11} contribution [18, 19, 20]. Despite the S_{11} dominance of the differential cross section, the nucleon polarization and photon asymmetry yield only small contributions from the S_{11} resonance. This illustrates beautifully how the polarization observables are the true discriminators of subtle dynamics. While the differential cross section is largely blind to all but the S_{11} contribution, the polarization observables show the intricacies of the dynamics in full color.

In Fig. 3 the solid line represents the full calculation employing both the S_{11} and D_{13} resonances together with the Born and vector meson terms. The dashed and long-dash short-dash lines represent employing only the S_{11} and D_{13} resonances, respectively. The dash-dot and dotted lines correspond to the calculation employing only the Born and vector meson terms, respectively. In contrast to the unpolarized differential cross section, the recoil nucleon polarization and the photon asymmetry are not dominated by the S_{11} but the D_{13} resonance makes the largest contribution. The S_{11} resonance, as well as the Born and vector meson terms, make significant contributions to the spin observables but through interference terms of the large S_{11} amplitude and the small ones coming from the other background components in the η photoproduction process. It is easy to note that the full calculation is significantly reduced with respect to the D_{13} calculation for the photon asymmetry due to these interference effects. These effects highlights the relevance of the polarization observables in studying the background processes in the η photoproduction process.

In Fig. 4 we show the polarization and asymmetry for neutron knockout. As for the case of proton knockout, all components of the elementary amplitude contributes significantly to the polarization observables specially through the interference terms which are stronger for the case of the neutron compared to that of the proton. Moreover, the D_{13} resonance makes the largest contribution for these observables. The branching ratios of the S_{11} and D_{13} resonances are 50% and 0.1%, respectively [6]. The sensitivity of the polarization observables to the D_{13} resonance is therefore striking in light of its small branching ratio. However, this sensitivity is very advantageous since the polarization observables therefore provide a unique opportunity to study the properties of this spin 3/2 resonance such as its off-shell effects which are believed to be very important [6]. Note that in both Figs. 3 and 4 the calculation employing only the vector meson exchange, results in the polarization being identically zero, hence no dotted line appears in either of these two figures for the polarization. The reason for this is that the "potential" resulting from only vector meson exchange is spin independent.

With respect to the Born terms, there are two uncertainties concerning the ηNN vertex: (i) the magnitude of the coupling constant and (ii) the type of coupling, i.e., pseudoscalar (PS) or pseudovector (PV) coupling. While for the πNN vertex there are convincing reasons, in terms of the low energy theorem and the approximate chiral symmetry of the $SU(2) \times SU(2)$ group, to oblige us to favor the PV over the PS coupling [52, 53], such considerations

are not necessarily valid for the ηNN vertex as a consequence of the largeness of the η mass and the significant breaking of the chiral $SU(3) \times SU(3)$ group [54, 55]. In Ref. [6] it is shown that an acceptable range for the ηNN coupling constant (g_η) is:

$$0.2 \leq g_\eta \leq 6.2. \quad (21)$$

In Fig. 5 we show calculations of the recoil nucleon polarization and the photon asymmetry for pseudoscalar and pseudovector coupling when the value of g_η is varied in the range specified in Eq. (21). The graphs on the left-hand-side (right-hand-side) are for PS (PV) coupling at the ηNN vertex. The values of the coupling constant chosen in the range specified above are shown on the graph of the polarization for pseudovector coupling. For the case of pseudoscalar (pseudovector) coupling, the polarization (asymmetry) is largely insensitive to variations in the value of g_η . When pseudovector coupling is employed, the polarization displays significant variations over the entire angular range. In fact, it systematically decreases with an increase in the value of g_η . Note that the asymmetry with pseudoscalar coupling has exactly the opposite behavior in that it decreases with a decrease in the value of g_η . In general the pseudovector coupling decreases the polarization for a fixed value of g_η . This decrease is more drastic the larger the value of g_η as can be seen by comparing the dotted line for the polarization for pseudoscalar and pseudovector coupling. The pseudovector coupling also tends to decrease the value of the photon asymmetry. The nonrelativistic analysis of Ref. [28] seems to indicate that the data favors a pseudoscalar coupling at the ηNN vertex. This is in contrast to the analysis of the elementary process in Ref. [6] where no conclusive evidence could be found for either type of coupling. However, caution must be exercised when comparing the two analyses, since the underlying dynamics are very different. Our results indicate that the magnitude of g_η also plays a role in investigating this ambiguity. To emphasize: the polarization is sensitive to the difference in the type of coupling when g_η is of the order of 3.0, 5.0 or 6.2.

B. Sensitivity to medium modifications of the resonance masses

In this section we investigate the sensitivity of the nucleon polarization and photon asymmetry to medium modifications of the masses of the S_{11} and D_{13} resonances. Since in the quasifree process the resonances propagate in the nuclear medium as opposed to free space,

one would expect changes to their physical properties such as effective masses. Now we examine the sensitivity of our observables to any possible medium modifications to these masses.

We consider proton knockout from the $1p^{3/2}$ orbital of ^{12}C with an incident photon energy of $E_\gamma = 750$ MeV and a missing momentum of $|\vec{p}_m| = 100$ MeV. For this calculation we used the Born and vector meson terms together with both resonances. In Fig. 6 the solid line corresponds to the free mass values, the dashed line a decrease of 3% and the long-dash short-dash line an increase of 3% in the masses of the S_{11} and D_{13} resonances. The graphs on the left-hand-side of Fig. 6 show the sensitivity of the polarization and the asymmetry to a change in the mass of the S_{11} resonance, whilst keeping the mass of the D_{13} resonance fixed. For the graphs on the right-hand-side, only the mass of the D_{13} resonance was varied.

The nucleon polarization shows little sensitivity over the entire angular range when only the mass of the S_{11} resonance is varied. The polarization is not sensitive to a decrease in the mass of the D_{13} resonance. An increase in the mass of D_{13} leads to a significant reduction relative to the free mass calculation for the polarization. The photon asymmetry does exhibit some sensitivity to a change in the mass of S_{11} . This observable is more sensitive to variations in the mass of D_{13} , in particular an increase. This confirms the findings of Ref. [28] that the photon asymmetry is a very useful observable to look for medium modifications for the resonances. Our results now indicate that in addition, the polarization is also sensitive to medium modifications to the mass of the D_{13} resonance.

C. Sensitivity to the nuclear target

In Fig. 7 we show results for the nucleon polarization and the photon asymmetry as a function of θ_η for a variety of nuclear targets. We considered valence proton knockout from the $1s^{1/2}$ orbital of ^4He , the $1p^{3/2}$ orbital of ^{12}C , the $1p^{1/2}$ orbital of ^{16}O , the $1d^{3/2}$ orbital of ^{40}Ca and the $3s^{1/2}$ orbital of ^{208}Pb . The incident photon energy was taken to be $E_\gamma = 750$ MeV and the missing momentum $|\vec{p}_m| = 100$ MeV. The calculations employed the Born and vector meson terms together with both the S_{11} and D_{13} resonances, as well as pseudoscalar coupling. The calculations clearly indicate that the nucleon polarization is practically target independent. This finding is in agreement with that of Ref. [32] (although for the kaon quasifree process). In the relativistic case the photon asymmetry does indeed

exhibit some dependence on the nuclear target although the sensitivity is rather small. The calculation for ^{12}C and ^4He coincide, while the photon asymmetry for ^{16}O , ^{40}Ca and ^{208}Pb are practically indistinguishable. The apparent independence of the polarization observables to nuclear target effects appears to be a feature shared by various meson photoproduction processes [32].

D. Unpolarized differential cross section as a measure of the momentum distribution of the wavefunction

The momentum distribution of the bound nucleon is customarily measured by doing electron scattering [33]. In this section we illustrate the remarkable similarity between the cross section and the momentum distribution of the bound nucleon for η photoproduction. In Fig. 8 we show the unpolarized cross section (solid line) as a function of the missing momentum for proton knockout from the $1p^{3/2}$ orbital of ^{12}C . The incident photon energy was taken to be $E_\gamma = 750$ MeV and the momentum transfer is fixed at $|\vec{q}| = 400$ MeV. For this calculation we have used the Born and vector meson terms together with both the S_{11} and D_{13} resonances. The dashed line represents the parameter E_α (up to an arbitrary scale) which is proportional to the momentum distribution of the bound proton wavefunction (see Eq. 19b). The similarity between the momentum distribution of the bound proton wavefunction and the cross section is undeniable. Beyond 300 MeV the cross section quickly tends to zero. A similar result was obtained in Ref. [32] for kaon photoproduction.

IV. CONCLUSIONS

In this paper we have studied quasifree η photoproduction via the calculation of the differential cross section, the recoil nucleon polarization and the photon asymmetry using a relativistic plane wave impulse approximation formalism. The emphasis was on the polarization observables since they are very sensitive to the underlying dynamics but largely insensitive to distortion and nuclear target effects. The use of a plane wave formalism greatly simplifies the calculation of the transition matrix element. Gardner and Piekarewicz showed in Ref. [36] that by introducing a bound-state propagator one can still write $|\mathcal{M}|^2$ in terms of traces over Dirac matrices. This not only allows one to use Feynman's trace techniques even

for quasifree scattering, but additionally results in analytical expressions for the spin observables. The boundstate wavefunction of the bound nucleon was calculated within a relativistic mean-field approximation to the Walecka model. For the elementary process we used the effective Lagrangian approach of Benmerrouche, Zhang, and Mukhopadhyay [6, 29, 30].

We investigated the sensitivity of the various observables to the elementary amplitude, medium modifications to the masses of the S_{11} and D_{13} resonances as well as nuclear target effects. Our results indicate that the nucleon polarization is practically target independent, whereas the asymmetry exhibits some small sensitivity. The polarization observables are very sensitive to the elementary amplitude. We find that, in contrast to coherent η photoproduction, the S_{11} resonance completely dominates the unpolarized cross section. However, the two spin observables are dominated by the background processes in the elementary amplitude and specially sensitive to the D_{13} resonance contribution. As a consequence, the polarization and asymmetry are considerably sensitive to variations in the mass of the D_{13} resonance. Indeed, a variation in the mass of this resonance leads to significant effects in the polarization and asymmetry. This finding agrees with the nonrelativistic analysis of Ref. [28]. The polarization and asymmetry are useful tools to study the two ambiguities at the ηNN vertex. The sensitivity of these observables to the magnitude of the coupling constant depends to a large extent on the type of coupling. The polarization (asymmetry) is insensitive to the magnitude of the coupling constant for pseudoscalar (pseudovector) coupling. However, the polarization (asymmetry) does indeed exhibit a sensitivity to the magnitude of the coupling constant for pseudovector (pseudoscalar) coupling.

The η photoproduction process shares many features with kaon photoproduction when viewed within a relativistic framework. There are several differences when compared to the findings of the nonrelativistic calculations for η photoproduction. A stark similarity, however, is that both formalism identify the polarization observables as the prime candidates to investigate medium modifications of the background processes such as the D_{13} resonance. Meanwhile, as a consequence of the large dominance in the differential cross section of the S_{11} resonance, the quasifree differential cross section provides an excellent tool to study medium modifications to the S_{11} resonance in order to distinguish between various models that attempt to understand the S_{11} resonance and its unique position as the lowest lying negative parity state in the baryon spectrum. The basic message of this article is now clear: to probe medium modifications to the S_{11} resonance, measure the differential cross section,

to study the background processes and their medium modifications, measure the polarization observables.

Acknowledgments

We are grateful to Professors M. Benmerrouche and A. J. Sarty for providing us with their model for the elementary amplitude. L. J. A. acknowledges the support of the Japan Society for the Promotion of Science and the United States National Science Foundation under award number 0002714. G.C.H acknowledges financial support from the Japanese Ministry of Education, Science and Technology for research conducted at the Research Center for Nuclear Physics, Osaka, Japan. This material is based upon work supported by the National Research Foundation under Grant numbers: GUN 2053786 (G.C.H), 2048567 (B.I.S.v.d.V).

- [1] C. B. Dover and P. M. Fishbane, Phys. Rev. Lett. **64**, 3115 (1990).
- [2] B. Krusche et al., Phys. Rev. Lett. **74**, 3736 (1995).
- [3] B. Krusche et al., Phys. Lett. **B358**, 40 (1995).
- [4] M. Benmerrouche and N. C. Mukhopadhyay, Phys. Rev. Lett. **67**, 1070 (1991).
- [5] Z.-p. Li, Phys. Rev. **D52**, 4961 (1995), nucl-th/9506033.
- [6] M. Benmerrouche, N. C. Mukhopadhyay, and J. F. Zhang, Phys. Rev. **D51**, 3237 (1995), hep-ph/9412248.
- [7] N. Kaiser, P. B. Siegel, and W. Weise, Phys. Lett. **B362**, 23 (1995), nucl-th/9507036.
- [8] C. Sauermann, B. L. Friman, and W. Norenberg, Phys. Lett. **B341**, 261 (1995), nucl-th/9408012.
- [9] D. Jido, N. Kodama, and M. Oka, Phys. Rev. **D54**, 4532 (1996), hep-ph/9604280.
- [10] H.-c. Kim and S. H. Lee, Phys. Rev. **D56**, 4278 (1997), nucl-th/9704035.
- [11] S. H. Lee and H.-c. Kim, Nucl. Phys. **A612**, 418 (1997), nucl-th/9608038.
- [12] D. Jido, M. Oka, and A. Hosaka, Phys. Rev. Lett. **80**, 448 (1998), hep-ph/9707307.
- [13] C. DeTar and T. Kunihiro, Phys. Rev. **D39**, 2805 (1989).
- [14] D. Jido, Y. Nemoto, M. Oka, and A. Hosaka, Nucl. Phys. **A671**, 471 (2000), hep-ph/9805306.

- [15] D. Jido, M. Oka, and A. Hosaka, *Prog. Theor. Phys.* **106**, 873 (2001), hep-ph/0110005.
- [16] H.-c. Kim, D. Jido, and M. Oka, *Nucl. Phys.* **A640**, 77 (1998), hep-ph/9806275.
- [17] M. Oka, private communication.
- [18] J. Piekarewicz, A. J. Sarty, and M. Benmerrouche, *Phys. Rev.* **C55**, 2571 (1997), nucl-th/9701019.
- [19] W. Peters, H. Lenske, and U. Mosel, *Nucl. Phys.* **A642**, 506 (1998), nucl-th/9807002.
- [20] L. J. Abu-Raddad, J. Piekarewicz, A. J. Sarty, and R. A. Rego, *Phys. Rev.* **C60**, 054606 (1999), nucl-th/9812061.
- [21] C. Bennhold and H. Tanabe, *Phys. Lett.* **B243**, 13 (1990).
- [22] D. Halderson and A. S. Rosenthal, *Phys. Rev.* **C42**, 2584 (1990).
- [23] R. C. Carrasco, *Phys. Rev.* **C48**, 2333 (1993).
- [24] L. Chen and H.-C. Chiang, *Phys. Lett.* **B329**, 424 (1994).
- [25] L. Tiator, C. Bennhold, and S. S. Kamalov, *Nucl. Phys.* **A580**, 455 (1994), nucl-th/9404013.
- [26] S. Barshay and A. Bramon, *Mod. Phys. Lett.* **A9**, 1727 (1994).
- [27] A. Hombach, A. Engel, S. Teis, and U. Mosel, *Z. Phys.* **A352**, 223 (1995), nucl-th/9411025.
- [28] F. X. Lee, L. E. Wright, C. Bennhold, and L. Tiator, *Nucl. Phys.* **A603**, 345 (1996), nucl-th/9601001.
- [29] M. Benmerrouche, Ph.D. thesis, Rensselaer Polytechnic Institute (1992).
- [30] N. C. Mukhopadhyay, J. F. Zhang, and M. Benmerrouche, *Phys. Lett.* **B364**, 1 (1995), hep-ph/9510307.
- [31] L. J. Abu-Raddad, Ph.D. thesis, Florida State University (2000), nucl-th/0005068.
- [32] L. J. Abu-Raddad and J. Piekarewicz, *Phys. Rev.* **C61**, 014604 (2000), nucl-th/9906066.
- [33] L. J. Abu-Raddad and J. Piekarewicz, *Phys. Rev.* **C64**, 064616 (2001), nucl-th/0106015.
- [34] X. Li, L. E. Wright, and C. Bennhold, *Phys. Rev.* **C48**, 816 (1993).
- [35] C. Bennhold, F. X. Lee, T. Mart, and L. E. Wright, *Nucl. Phys.* **A639**, 227c (1998), nucl-th/9712075.
- [36] S. Gardner and J. Piekarewicz, *Phys. Rev.* **C50**, 2822 (1994), nucl-th/9401001.
- [37] J. A. Caballero, T. W. Donnelly, E. Moya de Guerra, and J. M. Udias, *Nucl. Phys.* **A632**, 323 (1998), nucl-th/9710038.
- [38] V. Hejny et al., *Eur. Phys. J.* **A6**, 83 (1999).
- [39] V. Hejny et al., *Eur. Phys. J.* **A13**, 493 (2001).

- [40] M. Robig-Landau et al., Phys. Lett. **B373**, 45 (1996).
- [41] F. Mandl and G. Shaw, *Quantum Field Theory*, Wiley-Interscience Publication (Wiley, Chichester, UK, 1984), p 138.
- [42] R. Williams, C. R. Ji, and S. R. Cotanch, Phys. Rev. **D41**, 1449 (1990).
- [43] A. Nagl, V. Devanathan, and H. Überall, *Nuclear Pion Photoproduction*, vol. 120 of *Springer Tracts in Modern Physics* (Springer-Verlag, Berlin Heidelberg, Germany, 1991).
- [44] G. F. Chew, M. L. Goldberger, F. E. Low, and Y. Nambu, Phys. Rev. **106**, 1345 (1957).
- [45] C. Bennhold and H. Tanabe, Nucl. Phys. **A530**, 625 (1991).
- [46] S. Homma, M. Kanazawa, K. Maruyama, Y. Murata, H. Okuno, H. Sasaki, and T. Taniguchi, J. Phys. Soc. Jap. **57**, 828 (1988).
- [47] H. R. Hicks, S. R. Deans, D. T. Jacobs, P. W. Lyons, and D. L. Montgomery, Phys. Rev. **D7**, 2614 (1973), and references therein.
- [48] B. D. Serot and J. D. Walecka, Adv. Nucl. Phys. **16**, 1 (1986).
- [49] J. Sakurai, *Advanced Quantum Mechanics* (Addison-Wesley, 1973).
- [50] J. R. Taylor, *Scattering Theory: The Quantum Theory of Nonrelativistic Collisions* (John Wiley & Sons, 1972).
- [51] R. Mertig, M. Bohm, and A. Denner, Comput. Phys. Commun. **64**, 345 (1991), <http://www.feyncalc.org/>.
- [52] P. De Baenst, Nucl. Phys. **B24**, 633 (1970).
- [53] V. Bernard, N. Kaiser, and U. G. Meissner, Nucl. Phys. **B383**, 442 (1992).
- [54] M. Gell-Mann, R. J. Oakes, and B. Renner, Phys. Rev. **175**, 2195 (1968).
- [55] A. Manohar and H. Georgi, Nucl. Phys. **B234**, 189 (1984).

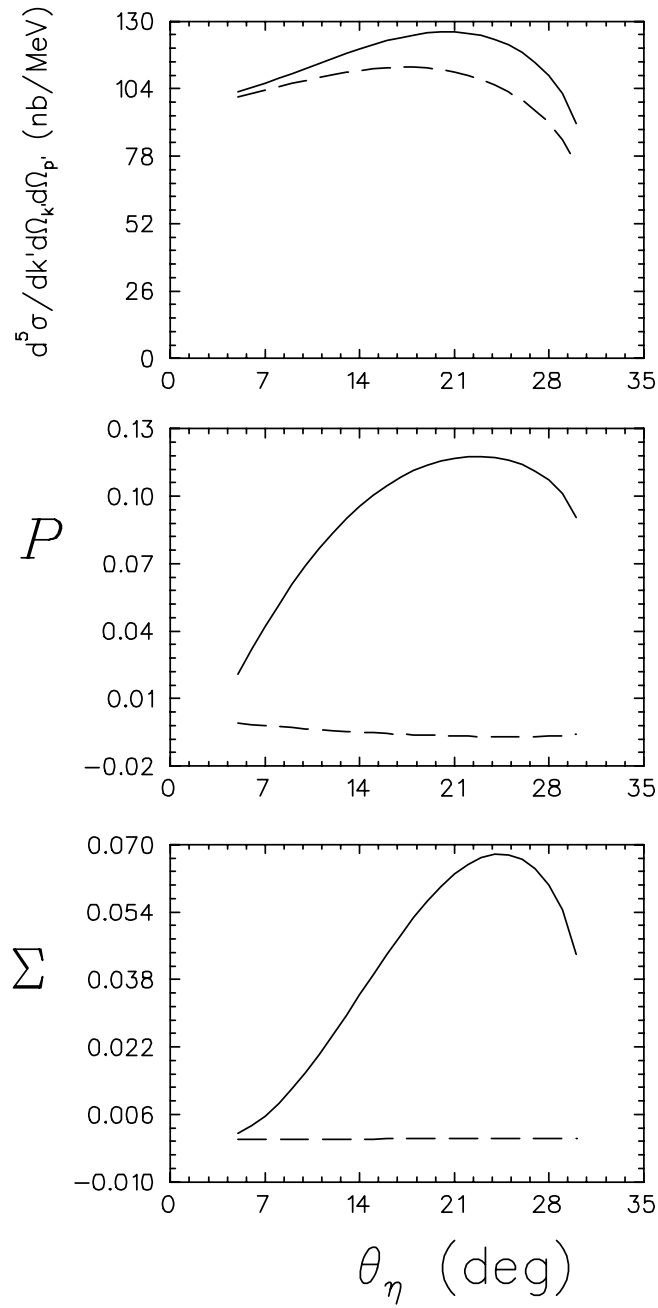


FIG. 2: Unpolarized differential cross section ($d^5\sigma/dk'd\Omega_{k'}d\Omega_{p'}$), recoil nucleon polarization (\mathcal{P}) and photon asymmetry (Σ) as a function of the η meson scattering angle θ_η for proton knockout from the $1p^{3/2}$ orbital of ^{12}C . The solid line represents the calculation using the Born and vector meson terms together with both the S_{11} and D_{13} resonances. The dashed line represents the calculations employing only the S_{11} resonance. The incident photon laboratory kinetic energy is $E_\gamma = 750$ MeV and the missing momentum is fixed at $|\vec{p}_m| = 100$ MeV.

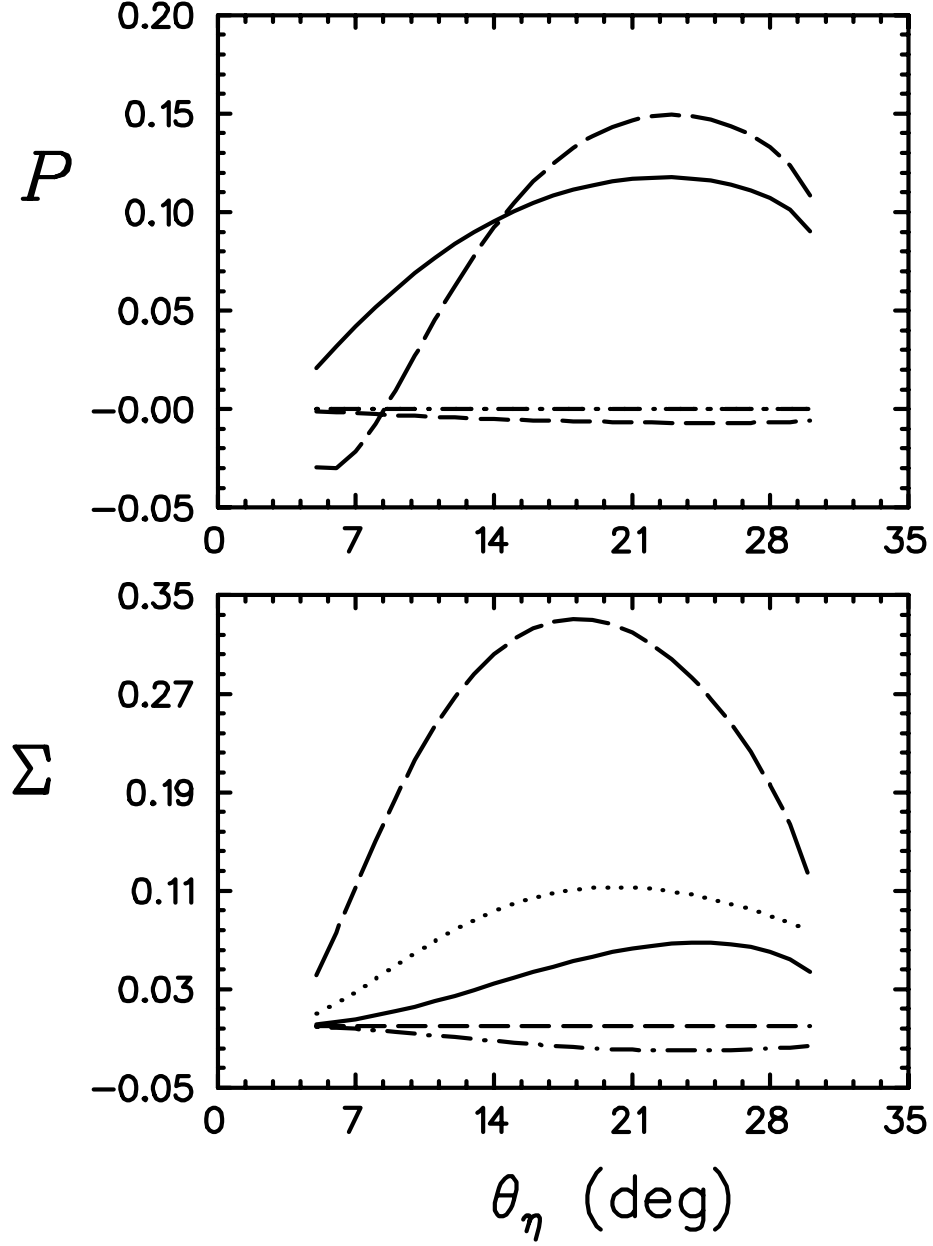


FIG. 3: The recoil nucleon polarization (\mathcal{P}) and the photon asymmetry (Σ) as a function of the η meson scattering angle (θ_η) for proton knockout from the $1p^{3/2}$ orbital of ^{12}C . The incident photon energy is $E_\gamma = 750$ MeV and the missing momentum is fixed at $|\vec{p}_m| = 100$ MeV. The solid line represents the full calculation employing both the S_{11} and D_{13} resonances together with the Born and vector meson terms. The dashed and long-dash short-dash lines represent employing only the S_{11} and D_{13} resonances, respectively. The dash-dot and dotted lines correspond to the calculation employing only the Born terms and vector meson terms, respectively.

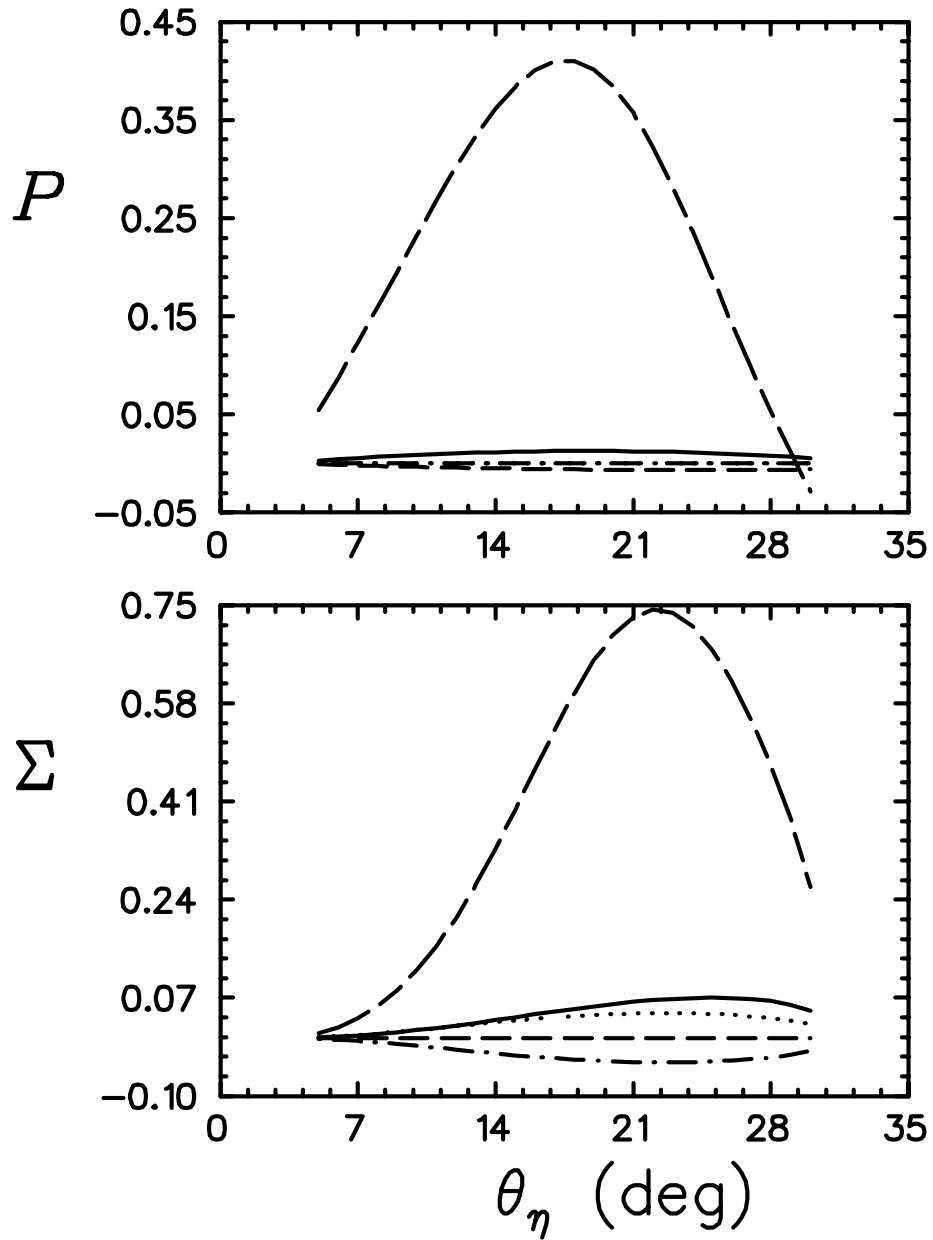


FIG. 4: The recoil nucleon polarization (\mathcal{P}) and the photon asymmetry (Σ) as a function of the η meson scattering angle (θ_η) for neutron knockout from the $1p^{3/2}$ orbital of ^{12}C . The incident photon energy is $E_\gamma = 750$ MeV and the missing momentum is fixed at $|\vec{p}_m| = 100$ MeV. The solid line represents the full calculation employing both the S_{11} and D_{13} resonances together with the Born and vector meson terms. The dashed and long-dash short-dash lines represent employing only the S_{11} and D_{13} resonances, respectively. The dash-dot and dotted lines correspond to the calculation employing only the Born terms and vector meson terms, respectively.

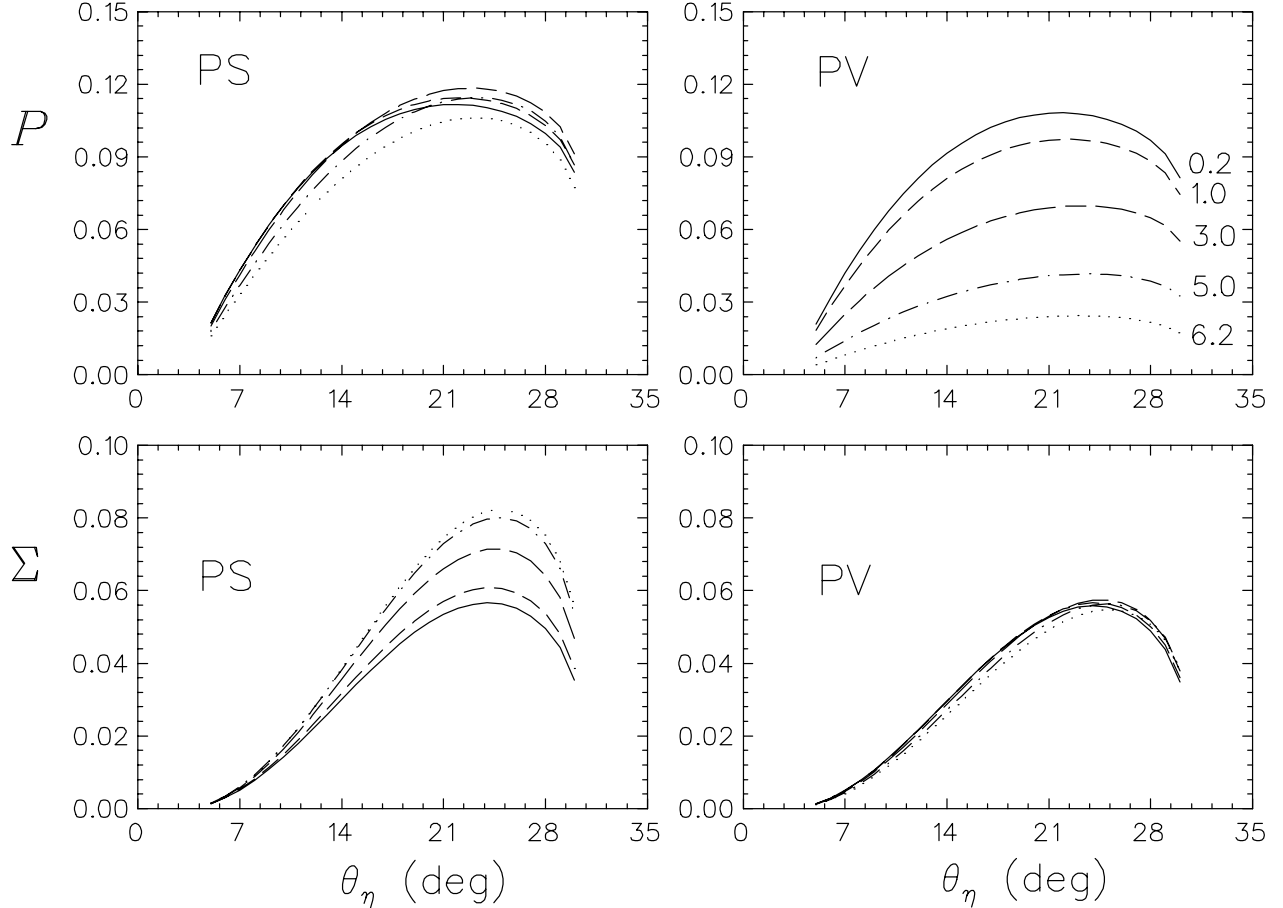


FIG. 5: Variation of the recoil nucleon polarization (\mathcal{P}) and the photon asymmetry (Σ) with respect to a change in the value of the η meson coupling constant (g_η) where $0.2 \leq g_\eta \leq 6.2$. The graphs on the left-hand-side (right-hand-side) are for PS (PV) coupling at the ηNN vertex. The values of the coupling constant chosen in the range specified above are shown on the graph of the polarization for pseudovector coupling. The calculations shown are for proton knockout from the $1p^{3/2}$ orbital of ^{12}C for an incident photon energy of 750 MeV and fixed missing momentum, $|\vec{p}_m| = 100$ MeV. The calculation employed both the S_{11} and D_{13} resonances together with the Born and vector meson terms.

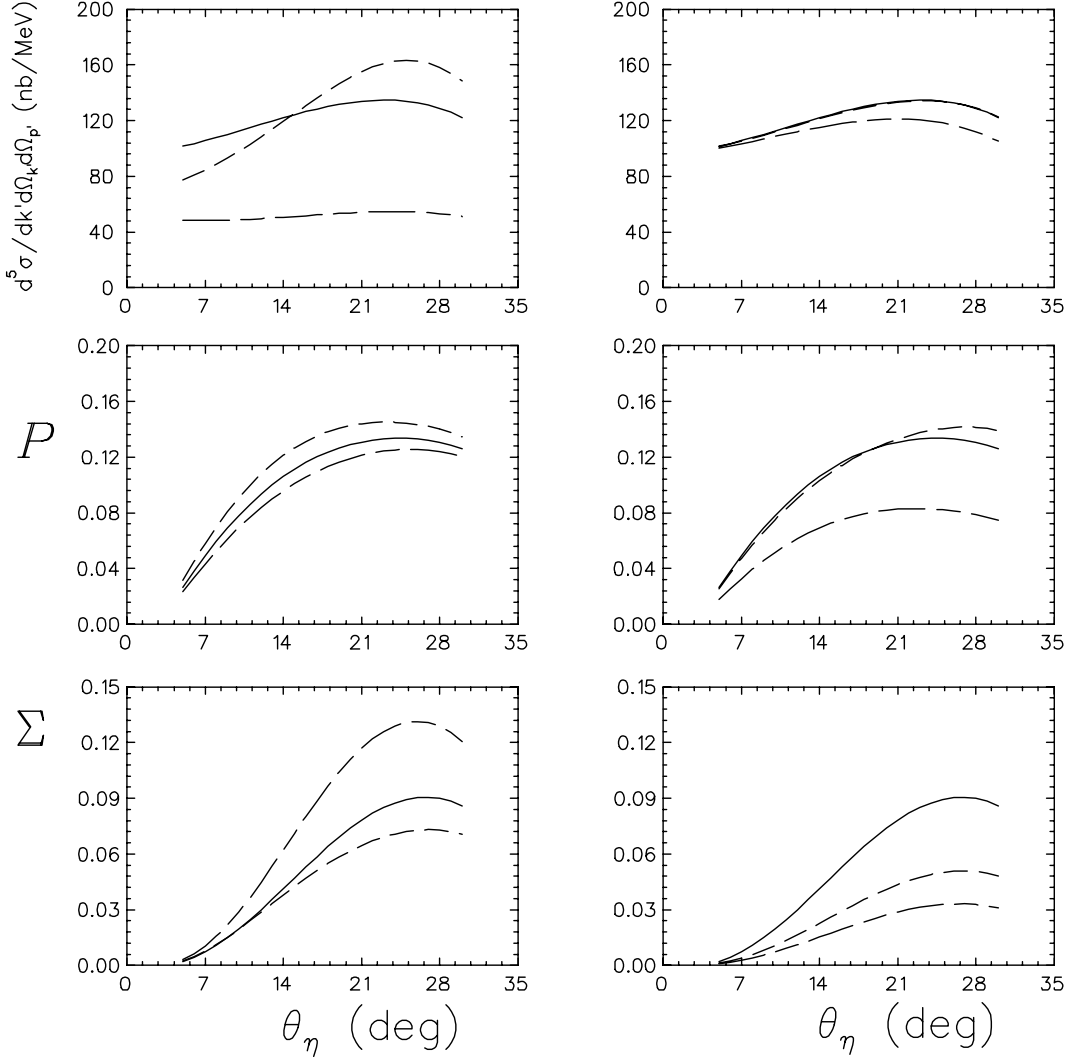


FIG. 6: Effect on the unpolarized differential cross section ($d^5\sigma/dk'd\Omega_k d\Omega_{p'}$), recoil nucleon polarization (P) and photon asymmetry (Σ) when the masses of the D_{13} and S_{11} resonances are increased (long-dash short-dash line) or decreased (dashed line) by 3%. The solid line corresponds to the free mass value for the two resonances. The results shown are for proton knockout from the $1p^{3/2}$ orbital of ^{12}C employing both resonances together with the Born and vector meson terms. The incident photon energy is $E_\gamma = 750$ MeV and the missing momentum is fixed at $|\vec{p}_m| = 100$ MeV. The graphs on the left-hand-side correspond to a variation in the mass of the S_{11} resonance, whilst keeping the mass of the D_{13} resonance fixed. The graphs on the right-hand-side correspond to a variation in only the mass of the D_{13} resonance.

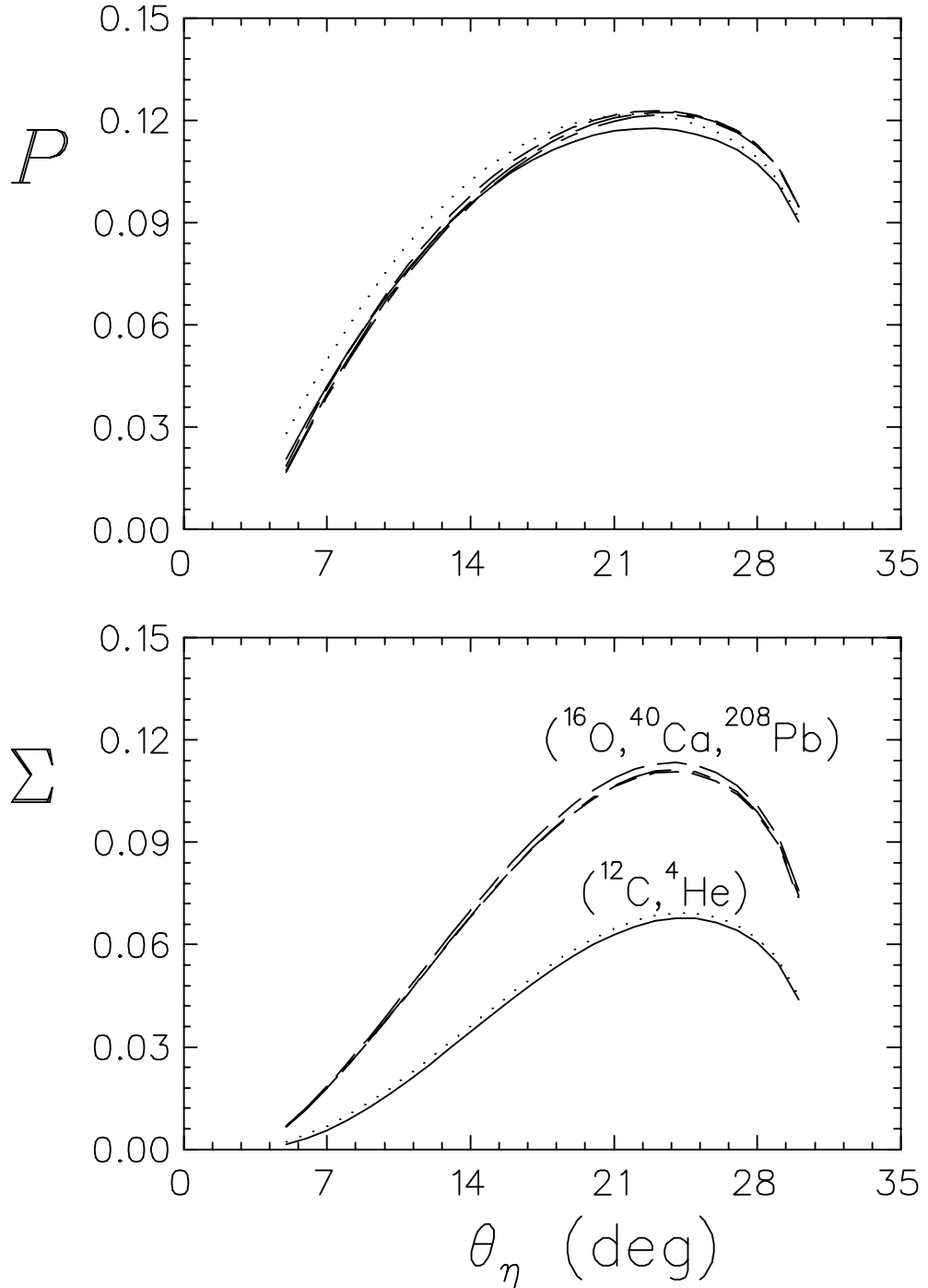


FIG. 7: Recoil nucleon polarization (\mathcal{P}) and photon asymmetry (Σ) for a variety of nuclear targets as a function of θ_η . The results shown are for the knockout of valence protons from the particular nucleus and employed both the S_{11} and D_{13} resonances together with the Born and vector meson terms. The incident photon energy is $E_\gamma = 750$ MeV and the missing momentum is $|\vec{p}_m| = 100$ MeV. The curves corresponding to a particular group of nuclei are shown on the graph of the asymmetry.

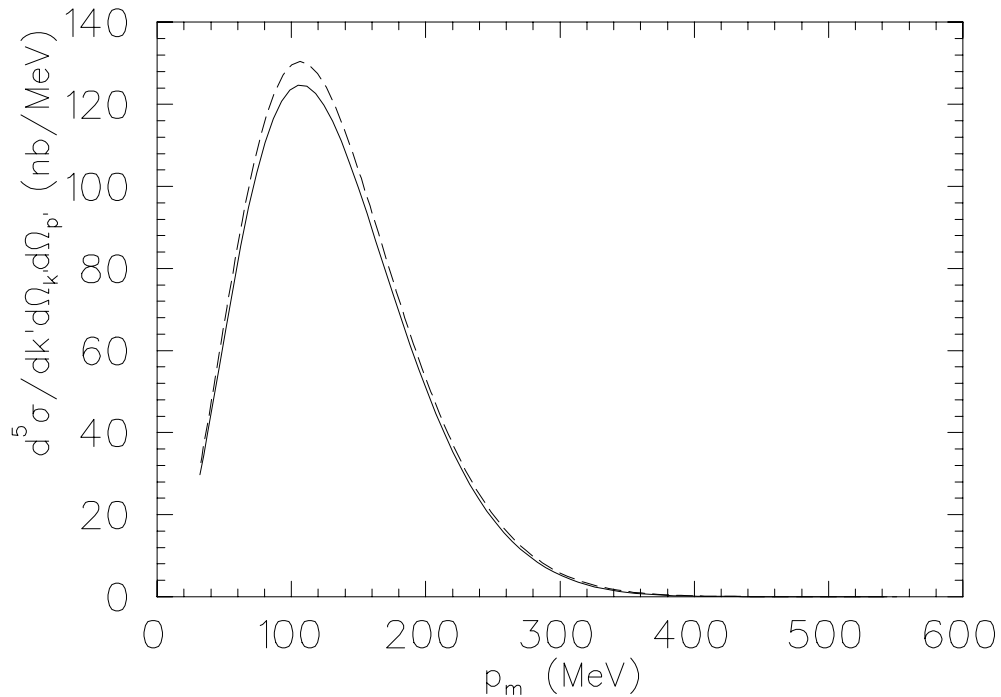


FIG. 8: The unpolarized differential cross section (solid line) as a function of the missing momentum for proton knockout from the $1p^{3/2}$ orbital of ^{12}C . The incident photon energy is $E_\gamma = 750$ MeV and the momentum transfer is fixed at $|\vec{q}| = 400$ MeV. The dashed line represents the parameter E_α (up to an arbitrary scale) which is proportional to the momentum distribution of the bound proton wavefunction.